Substitution of these expressions into Eq. 9.21 gives

$$\sigma_{rr} = \frac{M_x}{b}\left[\frac{d \ln\left(\frac{r}{a}\right) - (r-a)\ln\left(\frac{c}{a}\right)}{rd\left[R\ln\left(\frac{c}{a}\right) - d\right]}\right] \tag{a}$$

Maximizing σ_{rr} with respect to r, we find that $\sigma_{rr(\max)}$ occurs at

$$r = ae^{\left(1 - \frac{a}{d}\ln\frac{c}{a}\right)} \tag{b}$$

We evaluate Eq. (b) for the particular cross section of this example to obtain $r = 9.987$ m. At that location, the radial stress is, by Eq. (a),

$$\sigma_{rr(\max)} = \frac{202{,}500}{0.13}\left[\frac{0.80\ln\left(\frac{9.987}{9.6}\right) - \left[(9.987-9.6)\ln\left(\frac{10.4}{9.6}\right)\right]}{9.987(0.80)\left[10.0\ln\left(\frac{10.4}{9.6}\right) - 0.80\right]}\right] \tag{c}$$

$$= 0.292 \text{ MPa}$$

An approximate formula for computing radial stress in curved beams of rectangular cross section is (AITC, 1994, p. 227)

$$\sigma_{rr} = \frac{3M}{2Rbd} \tag{d}$$

Using this expression, we determine the radial stress to be $\sigma_{rr} = 0.292$ MPa. The approximation of Eq. (d) is quite accurate in this case! In fact, for rectangular curved beams with $R/d > 3$, the error in Eq. (d) is less than 3%. However, as R/d becomes small, the error grows substantially and Eq. (d) is nonconservative.

(b) Using the curved beam formula, Eq. 9.11, we obtain the maximum circumferential stress as $\sigma_{\theta\theta(\max)} = 15.0$ MPa. Using the straight-beam flexure formula, Eq. 7.1, with $I_x = bd^3/12 = 0.005547 \text{ m}^4$, we obtain $\sigma_{\theta\theta} = 202{,}500(0.40)/0.005547 = 14.6$ MPa. Thus, the straight-beam flexure formula is within 3% of the curved beam formula. One would generally consider the flexure formula adequate for this case, in which $R/d = 12.5$.

(c) The maximum circumferential stress is just within its limiting value; the beam is understressed just 5%. However, the maximum radial stress is 245% over its limit. It would be necessary to modify beam geometry or add mechanical reinforcement to make this design acceptable.

9.4 CORRECTION OF CIRCUMFERENTIAL STRESSES IN CURVED BEAMS HAVING I, T, OR SIMILAR CROSS SECTIONS

If the curved beam formula is used to calculate circumferential stresses in curved beams having thin flanges, the computed stresses are considerably in error and the error is nonconservative. The error arises because the radial forces developed in the curved beam causes the tips of the flanges to deflect radially, thereby distorting the cross section of the curved beam. The resulting effect is to decrease the stiffness of the curved beam, to decrease the circumferential stresses in the tips of the flanges, and to increase the circumferential stresses in the flanges near the web.

Consider a short length of a thin-flanged I-section curved beam included between faces *BC* and *FH* that form an infinitesimal angle $d\theta$ as indicated in Figure 9.6*a*. If the curved beam is subjected to a positive moment M_x, the circumferential stress distribution results in a tensile force *T* acting on the inner flange and a compressive force *C* acting on the outer flange, as shown. The components of these forces in the radial direction are $T\,d\theta$ and $C\,d\theta$. If the cross section of the curved beam did not distort, these forces would be uniformly distributed along each flange, as indicated in Figure 9.6*b*. However, the two portions of the tension and compression flanges act as cantilever beams fixed at the web. The resulting bending because of cantilever beam action causes the flanges to distort, as indicated in Figure 9.6*c*.

The effect of the distortion of the cross section on the circumferential stresses in the curved beam can be determined by examining the portion of the curved beam *ABCD* in Figure 9.6*d*. Sections *AC* and *BD* are separated by angle θ in the unloaded beam. When the curved beam is subjected to a positive moment, the center of curvature moves from 0 to 0*, section *AC* moves to *A*C**, section *BD* moves to *B*D**, and the included angle becomes θ^*. If the cross section does not distort, the inner tension flange *AB* elongates to length *A*B**. Since the tips of the inner flange move radially inward relative to the undistorted position (Figure 9.6*c*), the circumferential elongation of the tips of the inner flange is less than that indicated in Figure 9.6*d*. *Therefore,* $\sigma_{\theta\theta}$ *in the tips of the inner flange is less than that calculated using the curved beam formula.* To satisfy equilibrium, it is necessary that $\sigma_{\theta\theta}$ for the portion of the flange near the web be greater than that calculated using the curved beam formula. Now consider the outer compression flange. As indicated in Figure 9.6*d*, the outer flange shortens from *CD* to *C*D** if the cross section does not distort. Because of the distortion (Figure 9.6*c*), the tips of the compressive flange move radially outward, requiring less compressive contraction. *Therefore, the magnitude of* $\sigma_{\theta\theta}$

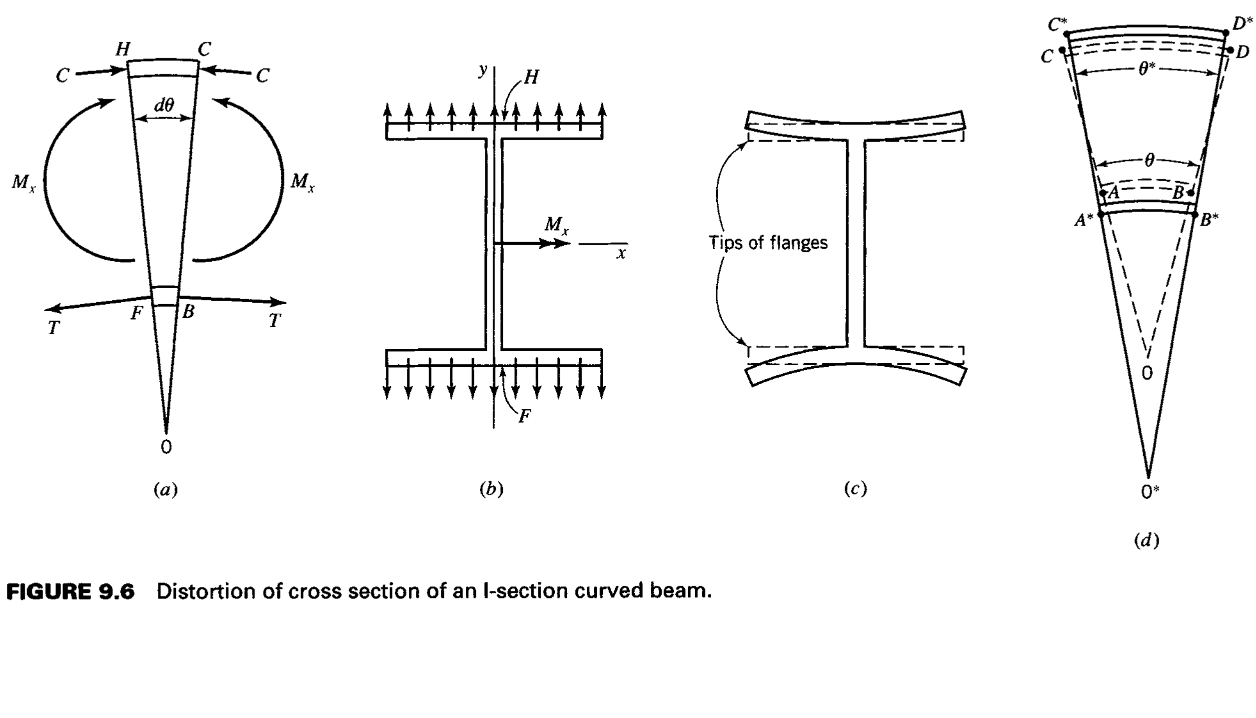

FIGURE 9.6 Distortion of cross section of an I-section curved beam.

in the tips of the compression outer flange is less than that calculated by the curved beam formula, and the magnitude of $\sigma_{\theta\theta}$ in the portion of the compression flange near the web is larger than that calculated by the curved beam formula.

The resulting circumferential stress distribution is indicated in Figure 9.7. Since in developing the curved beam formula we assume that the circumferential stress is independent of x (Figure 9.2), corrections are required if the formula is to be used in the design of curved beams having I, T, and similar cross sections. There are two approaches that can be employed in the design of these curved beams. One approach is to prevent the radial distortion of the cross section by welding radial stiffeners to the curved beams. If distortion of the cross section is prevented, the use of the curved beam formula is appropriate. A second approach, suggested by H. Bleich (1933), is discussed next.

9.4.1 Bleich's Correction Factors

Bleich reasoned that the actual maximum circumferential stresses in the tension and compression flanges for the I-section curved beam (Figure 9.8*a*) can be calculated by the curved beam formula applied to an I-section curved beam with *reduced flange widths*, as indicated in Figure 9.8*b*. By Bleich's method, if the same bending moment is applied to the two cross sections in Figure 9.8, the computed maximum circumferential tension and

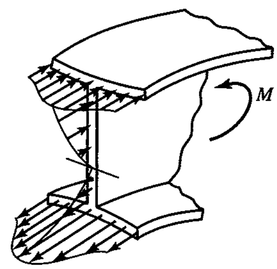

FIGURE 9.7 Stresses in I-section of curved beam.

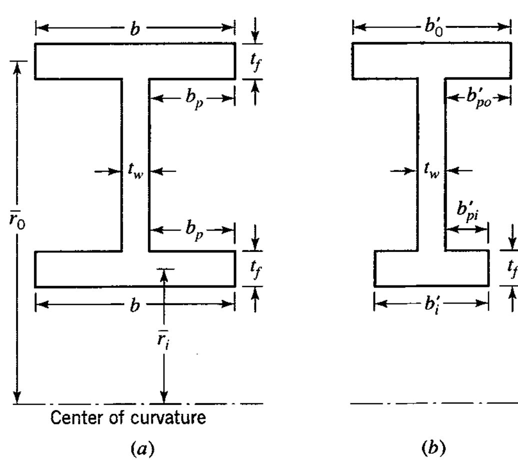

FIGURE 9.8 (*a*) Actual and (*b*) modified I-section for a curved beam.

compression stresses for the cross section shown in Figure 9.8*b*, with no distortion, are equal to the actual maximum circumferential tension and compression stresses for the cross section in Figure 9.8*a*, with distortion.

The approximate solution proposed by Bleich gives the results presented in tabular form in Table 9.3. To use the table, the ratio $b_p^2/\bar{r}t_f$ must be calculated, where

b_p = projecting width of flange (see Figure 9.8*a*)

$\bar{r}$ = radius of curvature to the center of flange

t_f = thickness of flange

The reduced width b_p' of the projecting part of each flange (Figure 9.8*b*) is given by the relation

$$b_p' = \alpha b_p \tag{9.22}$$

where α is obtained from Table 9.3 for the computed value of the ratio $b_p^2/\bar{r}t_f$. The reduced width of each flange (Figure 9.8*b*) is given by

$$b' = 2b_p' + t_w \tag{9.23}$$

where t_w is the thickness of the web. When the curved beam formula (Eq. 9.11) is applied to an undistorted cross section corrected by Eq. 9.23, it predicts the maxmum circumferential stress in the actual (distorted) cross section. This maximum stress occurs at the center of the inner flange. It should be noted that the state of stress at this point in the curved beam is not uniaxial. Because of the bending of the flanges (Figure 9.6*c*), a transverse component of stress σ_{xx} (Figure 9.2) is developed; the sign of σ_{xx} is opposite to that of $\sigma_{\theta\theta(\max)}$. Bleich obtained an approximate solution for σ_{xx} for the inner flange. It is given by the relation

$$\sigma_{xx} = -\beta\bar{\sigma}_{\theta\theta} \tag{9.24}$$

where β is obtained from Table 9.3 for the computed value of the ratio $b_p^2/\bar{r}t_f$, and where $\bar{\sigma}_{\theta\theta}$ is the magnitude of the circumferential stress at midthickness of the inner flange; the value of $\bar{\sigma}_{\theta\theta}$ is calculated based on the corrected cross section.

Although Bleich's analysis was developed for curved beams with relatively thin flanges, the results agree closely with a similar solution obtained by C. G. Anderson (1950) for I-beams and box beams, in which the analysis was not restricted to thin-flanged sections. Similar analyses of tubular curved beams with circular and rectangular cross

TABLE 9.3 Table for Calculating the Effective Width and Lateral Bending Stress of Curved I- or T-Beams

$b_p^2/\bar{r}t_f$	0.2	0.3	0.4	0.5	0.6	0.7	0.8	0.9	1.0
α	0.977	0.950	0.917	0.878	0.838	0.800	0.762	0.726	0.693
β	0.580	0.836	1.056	1.238	1.382	1.495	1.577	1.636	1.677
$b_p^2/\bar{r}t_f$	1.1	1.2	1.3	1.4	1.5	2.0	3.0	4.0	5.0
α	0.663	0.636	0.611	0.589	0.569	0.495	0.414	0.367	0.334
β	1.703	1.721	1.728	1.732	1.732	1.707	1.671	1.680	1.700

sections have been made by S. Timoshenko (1923). An experimental investigation by D. C. Broughton, M. E. Clark, and H. T. Corten (1950) showed that another type of correction is needed if the curved beam has extremely thick flanges and thin webs. For such beams each flange tends to rotate about a neutral axis of its own in addition to the rotation about the neutral axis of the curved beam cross section as a whole. Curved beams for which the circumferential stresses are appreciably increased by this action probably fail by excessive radial stresses.

Note: The radial stress can be calculated using either the original or the modified cross section.

EXAMPLE 9.8 *Bleich Correction Factors for T-Section*

A T-section curved beam has the dimensions indicated in Figure E9.8*a* and is subjected to pure bending. The curved beam is made of a steel having a yield stress $Y = 280$ MPa.

(a) Determine the magnitude of the moment that indicates yielding in the curved beam if Bleich's correction factors are not used.

(b) Use Bleich's correction factors to obtain a modified cross section. Determine the magnitude of the moment that initiates yielding for the modified cross section and compare with the result of part (a).

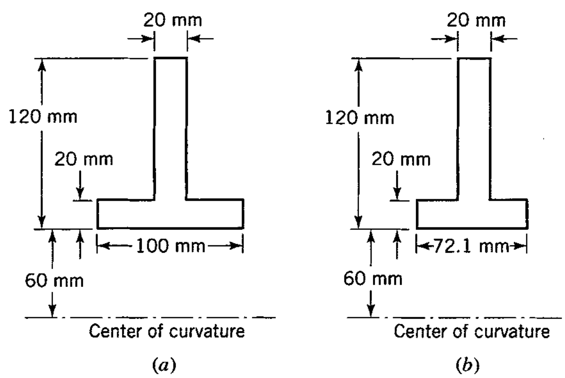

FIGURE E9.8 (*a*) Actual section. (*b*) Modified section.

Solution

(a) The magnitudes of A, A_m, and R for the actual cross section are given by Eqs. 9.12, 9.13, and 9.14, respectively, as follows: $A = 4000$ mm^2, $A_m = 44.99$ mm, and $R = 100.0$ mm. By comparison of the stresses at the locations $r = 180$ mm and $r = 60$ mm, we find that the maximum magnitude of $\sigma_{\theta\theta}$ occurs at the outer radius ($r = 180$ mm). (See Eq. 9.11.) Thus,

$$\sigma_{\theta\theta(\max)} = \left|\frac{M_x[4000 - 180(44.99)]}{4000(180)[100.0(44.9) - 4000]}\right|$$

$$= \left|-1.141 \times 10^{-5} M_x\right|$$

where M_x has the units of N • mm. Since the state of stress is assumed to be uniaxial, the magnitude of M_x to initiate yielding is obtained by setting $\sigma_{\theta\theta} = -Y$. Thus,

$$M_x = \frac{280}{1.141 \times 10^{-5}} = 24{,}540{,}000 \text{ N} \bullet \text{mm} = 24.54 \text{ kN} \bullet \text{m}$$

(b) The dimensions of the modified cross section are computed by Bleich's method; hence $b_p^2/\bar{r}t_f$ must be calculated. It is

$$\frac{b_p^2}{\bar{r}t_f} = \frac{40(40)}{70(20)} = 1.143$$

Linear interpolation in Table 9.3 yields $\alpha = 0.651$ and $\beta = 1.711$. Hence, by Eqs. 9.22 and 9.23, the modified flange width is $b_p' = \alpha b_p = 0.651(40) = 26.04$ mm and $b' = 2b_p' + t_w = 2(26.04) + 20 = 72.1$ mm (Figure E9.8*b*). For this cross section, by means of Eqs. 9.12, 9.13, and 9.14, we find

$$A = 72.1(20) + 20(100) = 3442 \text{ mm}^2$$

$$R = \frac{72.1(20)(70) + 20(100)(130)}{3442} = 104.9 \text{ mm}$$

$$A_m = 72.1 \ln\frac{80}{60} + 20 \ln\frac{180}{80} = 36.96 \text{ mm}$$

Now by means of Eq. 9.11, we find that the maximum magnitude of $\sigma_{\theta\theta}$ occurs at the inner radius of the modified cross section. Thus, with $r = 60$ mm, Eq. 9.11 yields

$$\sigma_{\theta\theta(\max)} = \frac{M_x[3442 - 60(36.96)]}{3442(60)[104.9(36.96) - 3442]} = 1.363 \times 10^{-5} M_x$$

The magnitude of M_x that causes yielding can be calculated by means of either the maximum shear stress criterion of failure or the octahedral shear stress criterion of failure. If the maximum shear stress criterion is used, the minimum principal stress must also be computed. The minimum principal stress is σ_{xx}. Hence, by Eqs. 9.11 and 9.24, we find

$$\bar{\sigma}_{\theta\theta} = \frac{M_x[3442 - 70(36.96)]}{3442(70)[104.9(36.96) - 3442]} = 8.15 \times 10^{-6} M_x$$

$$\sigma_{xx} = -\beta\bar{\sigma}_{\theta\theta} = -1.711(8.15 \times 10^{-6} M_x) = -1.394 \times 10^{-5} M_x$$

and

$$\tau_{\max} = \frac{\sigma_{\max} - \sigma_{\min}}{2} = \frac{Y}{2} = \frac{\sigma_{\theta\theta(\max)} - \sigma_{xx}}{2}$$

$$M_x = 10{,}140{,}000 \text{ N} \cdot \text{mm} = 10.14 \text{ kN} \cdot \text{m}$$

A comparison of the moment M_x determined in parts (a) and (b) indicates that the computed M_x required to initiate yielding is reduced by 58.8% because of the distortion of the cross section. Since the yielding is highly localized, its effect is not of concern unless the curved beam is subjected to fatigue loading. If the second principal stress σ_{xx} is neglected, the moment M_x is reduced by 16.5% because of the distortion of the cross section. The distortion is reduced if the flange thickness is increased.

9.5 DEFLECTIONS OF CURVED BEAMS

A convenient method for determining the deflections of a linearly elastic curved beam is by the use of Castigliano's theorem (Chapter 5). For example, the deflection and rotation of the free end of the curved beam in Figure 9.2*a* are given by the relations

$$\delta_{P_1} = \frac{\partial U}{\partial P_1} \tag{9.25}$$

$$\phi = \frac{\partial U}{\partial M_0} \tag{9.26}$$

where δ_{P_1} is the component of the deflection of the free end of the curved beam in the direction of load P_1, ϕ is the angle of rotation of the free end of the curved beam in the direction of M_0, and U is the total elastic strain energy in the curved beam. The total strain energy U (see Eq. 5.6) is equal to the integral of the strain-energy density U_0 over the volume of the curved beam (see Eqs. 3.33 and 5.7).

Consider the strain-energy density U_0 for a curved beam (Figure 9.2). Because of the symmetry of loading relative to the (y, z) plane, $\sigma_{xy} = \sigma_{xz} = 0$, and since the effect of the transverse normal stress σ_{xx} (Figure 9.2*b*) is ordinarily neglected, the formula for the strain-energy density U_0 reduces to the form

$$U_0 = \frac{1}{2E}\sigma_{\theta\theta}^2 + \frac{1}{2E}\sigma_{rr}^2 - \frac{v}{E}\sigma_{rr}\sigma_{\theta\theta} + \frac{1}{2G}\sigma_{r\theta}^2$$

where the radial normal stress σ_{rr}, the circumferential normal stress $\sigma_{\theta\theta}$, and the shear stress $\sigma_{r\theta}$ are, relative to the (x, y, z) axes of Figure 9.2*b*, $\sigma_{rr} = \sigma_{yy}$, $\sigma_{\theta\theta} = \sigma_{zz}$, and $\sigma_{r\theta} = \sigma_{yz}$. In addition, the effect of σ_{rr} is often small for curved beams of practical dimensions. Hence, the effect of σ_{rr} is often discarded from the expression for U_0. Then,

$$U_0 = \frac{1}{2E}\sigma_{\theta\theta}^2 + \frac{1}{2G}\sigma_{r\theta}^2$$

The stress components $\sigma_{\theta\theta}$ and $\sigma_{r\theta}$, respectively, contribute to the strain energies U_N and U_S because of the normal traction N and shear V (Figure 9.2*b*). In addition, $\sigma_{\theta\theta}$ contributes to the bending strain energy U_M, as well as to the strain energy U_{MN} because of a coupling effect between the moment M and traction N, as we shall see in the derivation below.

Ordinarily, it is sufficiently accurate to approximate the strain energies U_S and U_N that are due to shear V and traction N, respectively, by the formulas for straight beams (see Section 5.3). However, the strain energy U_M resulting from bending must be modified. To compute this strain energy, consider the curved beam shown in Figure 9.2*b*. Since the strain energy increment dU for a linearly elastic material undergoing small displacement is independent of the order in which loads are applied, let the shear load V and normal load N be applied first. Next, let the moment be increased from zero to M_x. The strain energy increment resulting from bending is

$$dU_M = \frac{1}{2}M_x\Delta(d\theta) = \frac{1}{2}M_x\omega\, d\theta \tag{9.27}$$

where $\Delta(d\theta)$, the change in $d\theta$, and $\omega = \Delta(d\theta)/d\theta$ are due to M_x alone. Hence, ω is determined from Eq. 9.10 with $N = 0$. Consequently, Eqs. 9.27 and Eq. 9.10 yield (with $N = 0$)

$$dU_M = \frac{A_m M_x^2}{2A(RA_m - A)E}\, d\theta \tag{9.28}$$

During the application of M_x, additional work is done by N because the centroidal (middle) surface (Figure 9.2*b*) is stretched an amount $d\bar{e}_{\theta\theta}$. Let the corresponding strain energy increment caused by the stretching of the middle surface be denoted by dU_{MN}. This strain energy increment dU_{MN} is equal to the work done by N as it moves through the distance $d\bar{e}_{\theta\theta}$. Thus,

$$dU_{MN} = Nd\bar{e}_{\theta\theta} = N\bar{\epsilon}_{\theta\theta}R\,d\theta \tag{9.29}$$

where $d\bar{e}_{\theta\theta}$ and $\bar{e}_{\theta\theta}$ refer to the elongation and strain of the centroidal axis, respectively. The strain $\bar{e}_{\theta\theta}$ is given by Eq. 9.3 with $r = R$. Thus, Eq. 9.3 (with $r = R$) and Eqs. 9.29, 9.9, and 9.10 (with $N = 0$) yield the strain energy increment dU_{MN} resulting from coupling of the moment M_x and traction N:

$$dU_{MN} = \frac{N}{E}\left[\frac{M_x}{RA_m - A} - R\frac{A_m M_x}{A(RA_m - A)}\right]d\theta = -\frac{M_x N}{EA}d\theta \tag{9.30}$$

By Eqs. 5.8, 5.14, 9.28, and 9.30, the total strain energy U for the curved beam is obtained in the form

$$U = U_S + U_N + U_M + U_{MN}$$

or

$$U = \int \frac{kV^2R}{2AG}d\theta + \int \frac{N^2R}{2AE}d\theta + \int \frac{A_m M_x^2}{2A(RA_m - A)E}d\theta - \int \frac{M_x N}{EA}d\theta \tag{9.31}$$

Equation 9.31 is an approximation, since it is based on the assumptions that plane sections remain plane and that the effect of the radial stress σ_{rr} on U is negligible. It might be expected that the radial stress increases the strain energy. Hence, Eq. 9.31 yields a low estimate of the actual strain energy. However, if M_x and N have the same sign, the coupling U_{MN}, the last term in Eq. 9.31, is negative. Ordinarily, U_{MN} is small and, in many cases, it is negative. Hence, we recommend that U_{MN}, the coupling strain energy, be discarded from Eq. 9.31 when it is negative. The discarding of U_{MN} from Eq. 9.31 raises the estimate of the actual strain energy when U_{MN} is negative and compensates to some degree for the lower estimate caused by discarding σ_{rr}.

The deflection δ_{elast} of rectangular cross section curved beams has been given by Timoshenko and Goodier (1970) for the two types of loading shown in Figure 9.4. The ratio of the deflection δ_U given by Castigliano's theorem and the deflection δ_{elast} is presented in Table 9.4 for several values of R/h. The shear coefficient k (see Eqs. 5.14 and 5.15) was taken to be 1.5 for the rectangular section, and Poisson's ratio ν was assumed to be 0.30.

TABLE 9.4 Ratios of Deflections in Rectangular Section Curved Beams Computed by Elasticity Theory and by Approximate Strain Energy Solution

	Neglecting U_{MN}		Including U_{MN}	
	Pure bending	Shear loading	Pure bending	Shear loading
$\left(\frac{R}{h}\right)$	$\left(\frac{\delta_U}{\delta_{elast}}\right)$	$\left(\frac{\delta_U}{\delta_{elast}}\right)$	$\left(\frac{\delta_U}{\delta_{elast}}\right)$	$\left(\frac{\delta_U}{\delta_{elast}}\right)$
0.65	0.923	1.563	0.697	1.215
0.75	0.974	1.381	0.807	1.123
1.0	1.004	1.197	0.914	1.048
1.5	1.006	1.085	0.968	1.016
2.0	1.004	1.048	0.983	1.008
3.0	1.002	1.021	0.993	1.003
5.0	1.000	1.007	0.997	1.001

Note: The deflection of curved beams is much less influenced by the curvature of the curved beam than is the circumferential stress $\sigma_{\theta\theta}$. If R/h is greater than 2.0, the strain energy resulting from bending can be approximated by that for a straight beam. Thus, for $R/h > 2.0$, for computing deflections the third and fourth terms on the right-hand side of Eq. 9.31 may be replaced by

$$U_M = \int \frac{M_x^2}{2EI_x} R\, d\theta \tag{9.32}$$

In particular, we note that the deflection of a rectangular cross section curved beam with $R/h = 2.0$ is 7.7% greater when the curved beam is assumed to be straight than when it is assumed to be curved.

9.5.1 Cross Sections in the Form of an I, T, etc.

As discussed in Section 9.4, the cross sections of curved beams in the form of an I, T, etc. undergo distortion when loaded. One effect of the distortion is to decrease the stiffness of the curved beam. As a result, deflections calculated on the basis of the undistorted cross section are less than the actual deflections. Therefore, the deflection calculations should be based on modified cross sections determined by Bleich's correction factors (Table 9.3). The strain energy terms U_N and U_M for the curved beams should also be calculated using the modified cross section. We recommend that the strain energy U_S be calculated with $k = 1.0$, and with the cross-sectional area A replaced by the area of the web $A_w = th$, where t is the thickness of the web and h is the curved beam depth. Also, as a working rule, we recommend that the coupling energy U_{MN} be neglected if it is negative and that it be doubled if it is positive.

EXAMPLE 9.9
Deformations in a Curved Beam Subjected to Pure Bending

The curved beam in Figure E9.9 is made of an aluminum alloy (E = 72.0 GPa), has a rectangular cross section with a thickness of 60 mm, and is subjected to a pure bending moment M = 24.0 kN • m.

(a) Determine the angle change between the two horizontal faces where M is applied.

(b) Determine the relative displacement of the centroids of the horizontal faces of the curved beam.

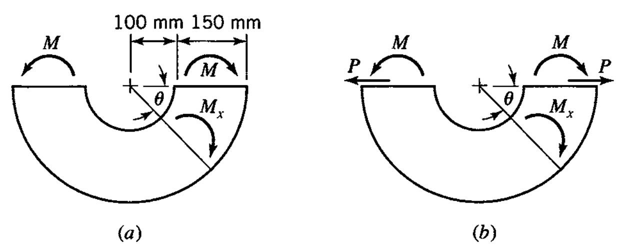

FIGURE E9.9

Solution

Required values for A, A_m, and R for the curved beam are calculated using equations in row (a) of Table 9.2:

$$A = 60(150) = 9000\ \text{mm}^2$$

$$A_m = 60 \ln\frac{250}{100} = 54.98\ \text{mm}$$

$$R = 100 + 75 = 175\ \text{mm}$$

(a) The angle change between the two faces where M is applied is given by Eq. 9.26. As indicated in Figure E9.9a, the magnitude of M_x at any angle θ is $M_x = M$. Thus, by Eq. 9.26, we obtain

$$\phi = \frac{\partial U}{\partial M} = \int_0^{\pi} \frac{A_m M_x}{A(RA_m - A)E}(1)\,d\theta$$
$$= \frac{54.98(24{,}000{,}000)\pi}{9000[175(54.98) - 9000](72{,}000)}$$
$$= 0.01029 \text{ rad}$$

(b) To determine the deflection of the curved beam, a load P must be applied as indicated in Figure E9.9b. In this case, $M_x = M + PR\sin\theta$ and $\partial U/\partial P = R\sin\theta$. Then the deflection is given by Eq. 9.25, in which the integral is evaluated with $P = 0$. Thus, the relative displacement is given by the relation

$$\delta_P = \frac{\partial U}{\partial P} = \int_0^{\pi} \frac{A_m M_x}{A(RA_m - A)E}\bigg|_{P=0}(R\sin\theta)\,d\theta$$

or

$$\delta_P = \frac{54.98(24{,}000{,}000)(175)(2)}{9000[175(54.98) - 9000](72{,}000)} = 1.147 \text{ mm}$$

EXAMPLE 9.10
Deflections in a Press

A press (Figure E9.10a) has the cross section shown in Figure E9.10b. It is subjected to a load P = 11.2 kN. The press is made of steel with E = 200 GPa and v = 0.30. Determine the separation of the jaws of the press caused by the load.

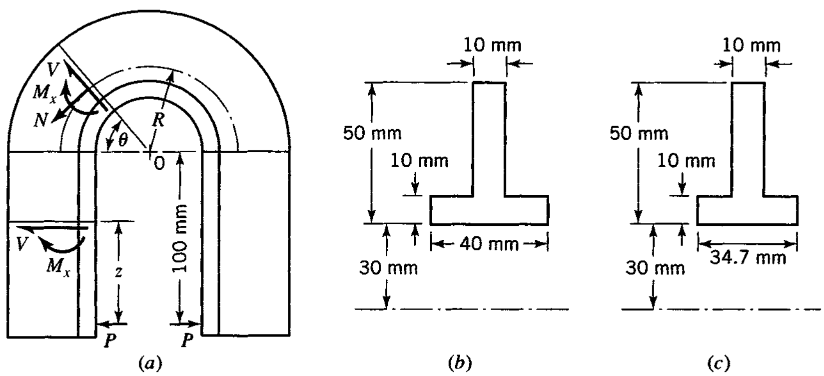

FIGURE E9.10 (*a*) Curved beam. (*b*) Actual section. (c) Modified section.

Solution

The press is made up of two straight members and a curved member. We compute the strain energies resulting from bending and shear in the straight beams, without modification of the cross sections. The moment of inertia of the cross section is $I_x = 181.7 \times 10^3$ mm^4. We choose the origin of the coordinate axes at load P, with z measured from P toward the curved beam. Then the applied shear V and moment M_x at a section in the straight beam are

$$V = P$$
$$M_x = Pz$$

In the curved beam portion of the press, we employ Bleich's correction factor to obtain a modified cross section. With the dimensions in Figure E9.10*b*, we find

$$\frac{b_p^2}{\bar{r}t_f} = \frac{15^2}{35(10)} = 0.643$$

A linear interpolation in Table 9.3 yields the result $\alpha = 0.822$. The modified cross section is shown in Figure E9.10*c*. Equations 9.12–9.14 give

$$A = 34.7(10) + 10(40) = 747 \text{ mm}^2$$

$$R = \frac{34.7(10)(35) + 10(40)(60)}{747} = 48.4 \text{ mm}$$

$$A_m = 10 \ln\frac{80}{40} + 34.7 \ln\frac{40}{30} = 16.9 \text{ mm}$$

With θ defined as indicated in Figure E9.10*a*, the applied shear V, normal load N, and moment M_x for the curved beam are

$$V = P\cos\theta$$
$$N = P\sin\theta$$
$$M_x = P(100 + R\sin\theta)$$

Summing the strain energy terms for the two straight beams and the curved beam and taking the derivative with respect to P (Eq. 9.25), we compute the increase in distance δ_P between the load points as

$$\delta_P = 2\int_0^{100} \frac{P}{A_w G} dz + 2\int_0^{100} \frac{Pz^2}{EI_x} dz + \int_0^{\pi} \frac{P\cos^2\theta}{A_w G} R\,d\theta + \int_0^{\pi} \frac{P\sin^2\theta}{AE} R\,d\theta + \int_0^{\pi} \frac{P(100 + R\sin\theta)^2 A_m}{A(RA_m - A)E} d\theta$$

The shear modulus is $G = E/[2(1 + \nu)] = 76{,}900$ MPa and $A_w = th = (10)(50) = 500 \text{ mm}^2$. Hence,

$$\delta_P = \frac{2(11{,}200)(100)}{76{,}900(500)} + \frac{2(11{,}200)(100)^3}{3(200{,}000)(181{,}700)}$$
$$+ \frac{11{,}200(48.4)\pi}{500(76{,}900)(2)} + \frac{11{,}200(48.4)\pi}{747(200{,}000)(2)}$$
$$+ \frac{16.9(11{,}200)}{747[48.4(16.9) - 747](200{,}000)}\left[(100)^2\pi + \frac{\pi}{2}(48.4)^2 + 2(100)(48.4)(2)\right]$$

or

$$\delta_P = 0.058 + 0.205 + 0.022 + 0.006 + 0.972 = 1.263 \text{ mm}$$

9.6 STATICALLY INDETERMINATE CURVED BEAMS: CLOSED RING SUBJECTED TO A CONCENTRATED LOAD

Many curved members, such as closed rings and chain links, are statically indeterminate (see Section 5.5). For such members, equations of equilibrium are not sufficient to determine all the internal resultants (V, N, M_x) at a section of the member. The additional relations needed to solve for the loads are obtained using Castigliano's theorem with appropriate boundary conditions. Since closed rings are commonly used in engineering, we present the computational procedure for a closed ring.

Consider a closed ring subjected to a central load P (Figure 9.9*a*). From the condition of symmetry, the deformations of each quadrant of the ring are identical. Hence, we need consider only one quadrant. The quadrant (Figure 9.9*b*) may be considered fixed at section FH with a load $P/2$ and moment M_0 at section BC. Because of the symmetry of the ring, as the ring deforms, section BC remains perpendicular to section FH. Therefore, by Castigliano's theorem, we have for the rotation of face BC

$$\phi_{BC} = \frac{\partial U}{\partial M_0} = 0 \tag{9.33}$$

The applied loads V, N, and M_x at a section forming angle θ with the face BC are

$$\begin{aligned} V &= \frac{P}{2}\sin\theta \\ N &= \frac{P}{2}\cos\theta \\ M_x &= M_0 - \frac{PR}{2}(1-\cos\theta) \end{aligned} \tag{9.34}$$

Substituting Eqs. 9.31 and 9.34 into Eq. 9.33, we find

$$0 = \int_0^{\pi/2} \frac{\left[M_0 - \left(\frac{PR}{2}\right)(1-\cos\theta)\right]A_m}{A(RA_m - A)E}\,d\theta - \int_0^{\pi/2} \frac{\left(\frac{P}{2}\right)\cos\theta}{AE}\,d\theta \tag{9.35}$$

where U_{MN} has been included. The solution of Eq. 9.35 is

$$M_0 = \frac{PR}{2}\left(1 - \frac{2A}{RA_m\pi}\right) \tag{9.36}$$

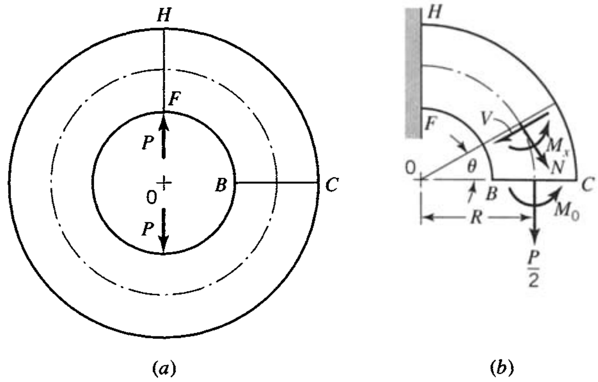

FIGURE 9.9 Closed ring.

If R/h is greater than 2.0, we take the bending energy U_M as given by Eq. 9.32 and ignore the coupling energy U_{MN}. Then, M_0 is given by the relation

$$M_0 = \frac{PR}{2}\left(1 - \frac{2}{\pi}\right) \tag{9.37}$$

With M_0 known, the loads at every section of the closed ring (Eqs. 9.34) are known. The stresses and deformations of the closed ring may be calculated by the methods of Sections 9.2–9.5.

9.7 FULLY PLASTIC LOADS FOR CURVED BEAMS

In this section we consider curved beams made of elastic–perfectly plastic materials with yield stress Y (Figure 1.5*b*). For a curved beam made of elastic–perfectly plastic material, the fully plastic moment M_P under pure bending is the same as that for a straight beam with identical cross section and material. However, because of the nonlinear distribution of the circumferential stress $\sigma_{\theta\theta}$ in a curved beam, the ratio of the fully plastic moment M_P under pure bending to maximum elastic moment M_Y is much greater for a curved beam than for a straight beam with the same cross section.

Most curved beams are subjected to complex loading other than pure bending. The stress distribution for a curved beam at the fully plastic load P_P for a typical loading condition is indicated in Figure 9.10. Since the tension stresses must balance the compression stresses and load P_P, the part A_T of the cross-sectional area A that has yielded in tension is larger than the part A_C of area A that has yielded in compression. In addition to the unknowns A_T and A_C, a third unknown is P_P, the load at the fully plastic condition. This follows because R (the distance from the center of curvature 0 to the centroid $\bar{0}$) can be calculated and D is generally specified rather than P_P. The three equations necessary to determine the three unknowns A_T, A_C, and P_P are obtained from the equations of equilibrium and the fact that the sum of A_T and A_C must equal the cross-sectional area A, that is,

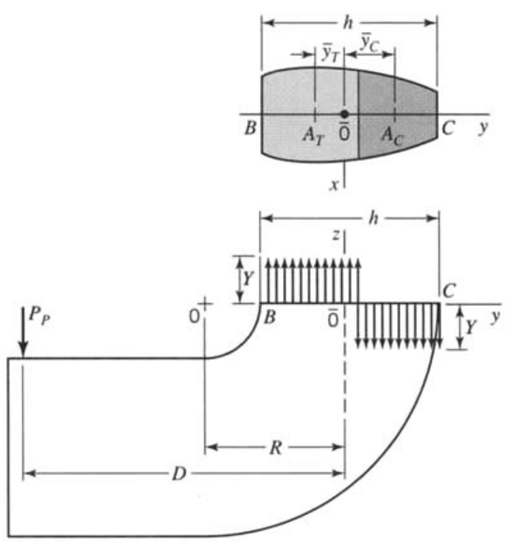

FIGURE 9.10 Stress distribution for a fully plastic load on a curved beam.

$$A = A_T + A_C \tag{9.38}$$

The equilibrium equations are (Figure 9.10)

$$\sum F_z = 0 = A_T Y - A_C Y - P_P \tag{9.39}$$

$$\sum M_x = 0 = P_P D - A_T Y \bar{y}_T - A_C Y \bar{y}_C \tag{9.40}$$

In Eq. 9.40, $\bar{y}_T$ and $\bar{y}_C$ locate the centroids of A_T and A_C, respectively, as measured from the centroid $\bar{0}$ of the cross-sectional area of the curved beam (Figure 9.10). Let M be the moment, about the centroidal axis x, resulting from the stress distribution on section BC (Figure 9.10). Then,

$$M = P_P D = A_T Y \bar{y}_T + A_C Y \bar{y}_C \tag{9.41}$$

Trial and error can be used to solve Eqs. 9.38–9.40 for the magnitudes of A_T, A_C, and P_P, since $\bar{y}_T$ and $\bar{y}_C$ are not known until A_T and A_C are known (McWhorter et al., 1971).

The moment M (Eq. 9.41) is generally less than the fully plastic moment M_P for pure bending. It is desirable to know the conditions under which M resulting from load P_P can be assumed equal to M_P, since for pure bending A_T is equal to A_C, and the calculations are greatly simplified. For some common sections, $M \approx M_P$, when $D > h$. For example, for $D = h$, we note that $M = 0.94M_P$ for curved beams with rectangular sections and $M = 0.96M_P$ for curved beams with circular sections. However, for curved beams with T-sections, M may be greater than M_P. Other exceptions are curved beams with I-sections and box-sections, for which D should be greater than $2h$ for M to be approximately equal to M_P.

9.7.1 Fully Plastic Versus Maximum Elastic Loads for Curved Beams

A linearly elastic analysis of a load-carrying member is required to predict the load–deflection relation for linearly elastic behavior of the member up to the load P_Y that initiates yielding in the member. The fully plastic load is also of interest since it is often considered to be the limiting load that can be applied to the member before the deformations become excessively large.

The fully plastic load P_P for a curved beam is often more than twice the maximum elastic load P_Y. Fracture loads for curved beams that are made of ductile metals and subjected to static loading may be four to six times P_Y. Dimensionless load–deflection experimental data for a uniform rectangular section hook made of a structural steel are shown in Figure 9.11. The deflection is defined as the change in distance ST between points S and T on the hook. The hook does not fracture even for loads such that $P/P_Y > 5$. A computer program written by J. C. McWhorter, H. R. Wetenkamp, and O. M. Sidebottom (1971) gave the predicted curve in Figure 9.11. The experimental data agree well with predicted results.

As noted in Figure 9.11, the ratio of P_P to P_Y is 2.44. Furthermore, the load–deflection curve does not level off at the fully plastic load but continues to rise. This behavior may be attributed to strain hardening. Because of the steep stress gradient in the hook, the strains in the most strained fibers become so large that the material begins to strain harden before yielding can penetrate to sufficient depth at section BC in the hook to develop the fully plastic load.

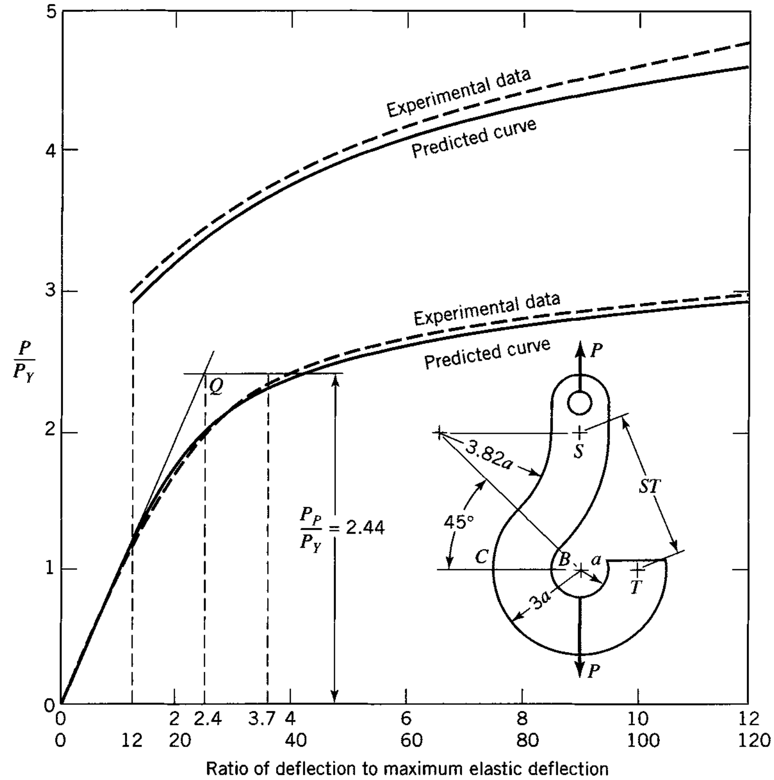

FIGURE 9.11 Dimensionless load–deflection curves for a uniform rectangular section hook made of structural steel.

The usual practice in predicting the deflection of a structure at the fully plastic load is to assume that the structure behaves in a linearly elastic manner up to the fully plastic load (point Q in Figure 9.11) and multiply the deflection at this point by the ratio P_P/P_Y (in this case, 2.44). In this case, with this procedure (Figure 9.11) the resulting calculated deflection [approximately calculated as 2.44(2.4) = 5.9] is greater than the measured deflection.

Usually, curved members such as crane hooks and chains are not subjected to a sufficient number of repetitions of peak loads during their life for fatigue failure to occur. Therefore, the working loads for these members are often obtained by application of a factor of safety to the fully plastic loads. It is not uncommon to have the working load as great as or greater than the maximum elastic load P_Y.

PROBLEMS

Section 9.2

9.1. A curved beam has the T-shaped cross section shown in Figure P9.1. The radius of curvature to the inner face of the flange is 20 mm. The maximum allowable circumferential stress has a magnitude of 250 MPa. Determine the magnitude of the bending moment that may be applied to the beam.

9.2. A curved steel bar of circular cross section is used as a crane hook (Figure P9.2). The radius of curvature to the inner edge of the bar is r and the bar has diameter d.

a. Determine the maximum tensile and compressive stresses at section A–A in terms of load P, radius r, and diameter d.

b. The maximum allowable design tensile stress at section A–A is 375 MPa. Determine the maximum allowable load P, for a radius r = 75 mm and a diameter d = 50 mm.

9.3. In a redesign of the aircraft beam of Example 9.2, the beam is replaced by a beam with the cross section shown in Figure P9.3.

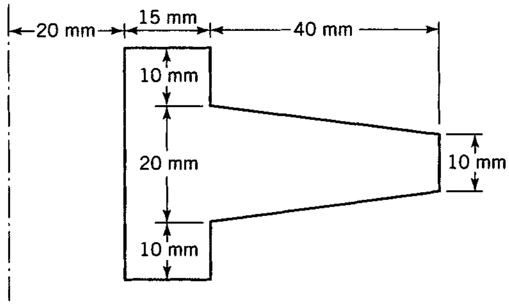

FIGURE P9.1

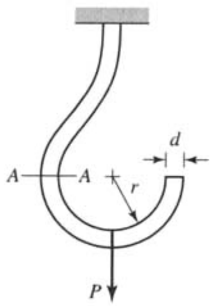

FIGURE P9.2

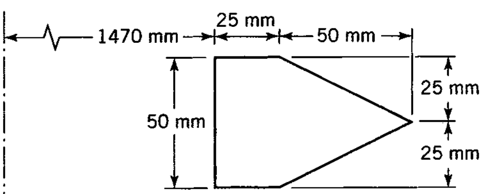

FIGURE P9.3

a. Rework Example 9.2 with the new cross section.

b. Compare the results to those of Example 9.2.

c. Comment on the worthiness of the redesign.

9.4. Rework Example 9.4 assuming that the pin exerts a uniform pressure p on the hook at radius r_i for $0 \leq \theta \leq \pi$. Compare the results to those of Example 9.4.

9.5. The frame shown in Figure E9.1 has a rectangular cross section with a thickness of 10 mm and depth of 40 mm. The load P is located 120 mm from the centroid of section BC. The frame is made of steel having a yield stress of Y = 430 MPa. The frame has been designed using a factor of safety of SF = 1.75 against initiation of yielding. Determine the maximum allowable magnitude of P, if the radius of curvature at section BC is R = 40 mm.

9.6. Solve Problem 9.5 for the condition that R = 35 mm.

9.7. The curved beam in Figure P9.7 has a circular cross section 50 mm in diameter. The inside diameter of the curved beam is 40 mm. Determine the stress at B for P = 20 kN.

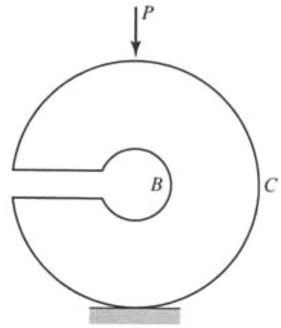

FIGURE P9.7

9.8. Let the crane hook in Figure E9.3 have a trapezoidal cross section as shown in row (c) of Table 9.2 with (see Figure P9.8) a = 45 mm, c = 80 mm, b_1 = 25 mm, and b_2 = 10 mm. Determine the maximum load to be carried by the hook if the working stress limit is 150 MPa.

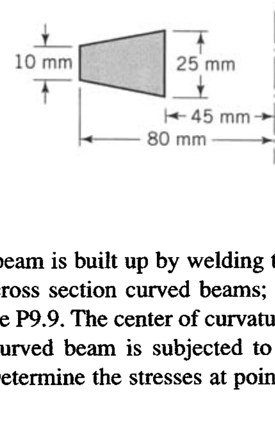

FIGURE P9.8

9.9. A curved beam is built up by welding together rectangular and elliptical cross section curved beams; the cross section is shown in Figure P9.9. The center of curvature is located 20 mm from B. The curved beam is subjected to a positive bending moment M_x. Determine the stresses at points B and C in terms of M_x.

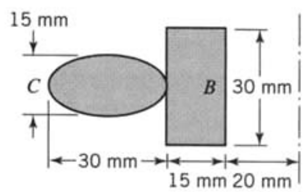

FIGURE P9.9

9.10. A commercial crane hook has the cross-sectional dimensions shown in Figure P9.10 at the critical section that is subjected to an axial load P = 100 kN. Determine the circumferential stresses at the inner and outer radii for this load.

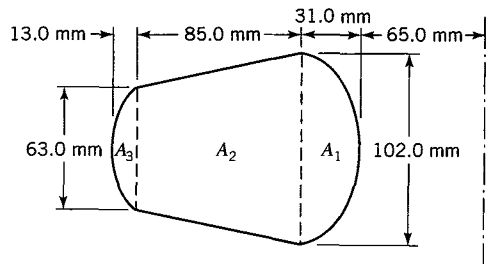

FIGURE P9.10

Assume that area A_1 is half of an ellipse [see row (j) in Table 9.2] and area A_3 is enclosed by a circular arc.

9.11. A crane hook has the cross-sectional dimensions shown in Figure P9.11 at the critical section that is subjected to an axial load $P = 90.0$ kN. Determine the circumferential stresses at the inner and outer radii for this load. Note that A_1 and A_3 are enclosed by circular arcs.

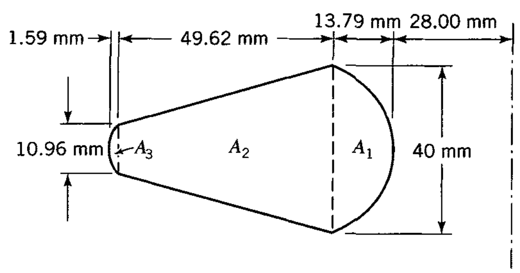

FIGURE P9.11

9.12. The curved beam in Figure P9.12 has a triangular cross section with the dimensions shown. If $P = 40$ kN, determine the circumferential stresses at B and C.

Section 9.3

9.14. Determine the distribution of the radial stress σ_{rr} in section BC of the beam of Example 9.1. Also determine the maximum value of σ_{rr} and its location.

9.15. Determine the magnitude of the radial stress σ_{rr} in section BC of Figure P9.12 at a radial distance of 30 mm from point B.

9.16. For the curved beam in Problem 9.9, determine the radial stress in terms of the moment M_x if the thickness of the web at the weld is 10 mm.

9.17. Figure P9.17 shows a cast iron frame with a U-shaped cross section. The ultimate tensile strength of the cast iron is $\sigma_u = 320$ MPa.

a. Determine the maximum value of P based on a factor of safety $SF = 4.00$, which is based on the ultimate strength.

b. Neglecting the effect of stress concentrations at the fillet at the junction of the web and flange, determine the maximum radial stress when this load is applied.

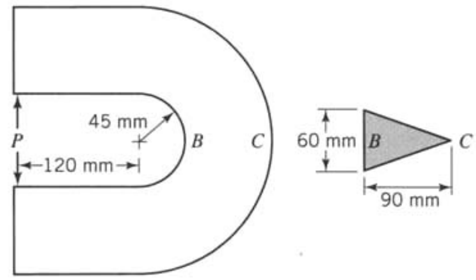

FIGURE P9.12

9.13. A curved beam with a rectangular cross section strikes a 90° arc and is loaded and supported as shown in Figure P9.13. The thickness of the beam is 50 mm. Determine the hoop stress $\sigma_{\theta\theta}$ along line A–A at the inside and outside radii and at the centroid of the beam.

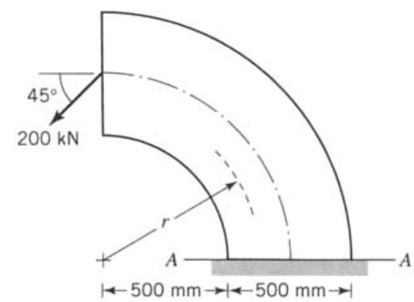

FIGURE P9.13

c. Is the maximum radial stress less than the maximum circumferential stress?

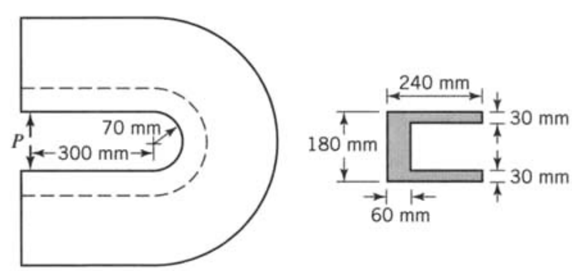

FIGURE P9.17

Section 9.4

9.18. A T-section curved beam has the cross section shown in Figure P9.18. The center of curvature lies 40 mm from the flange. If the curved beam is subjected to a positive bending moment $M_x = 2.50$ kN • m, determine the stresses at the inner and outer radii. Use Bleich's correction factors. What is the maximum shear stress in the curved beam?

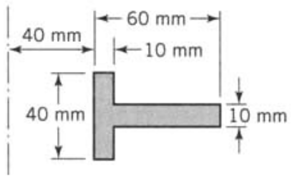

FIGURE P9.18

9.19. Determine the radial stress at the junction of the web and the flange for the curved beam in Problem 9.18. Neglect stress concentrations. Use the Bleich correction.

9.20. A load $P = 12.0$ kN is applied to the clamp shown in Figure P9.20. Determine the circumferential stresses at points B and C, assuming that the curved beam formula is valid at that section.

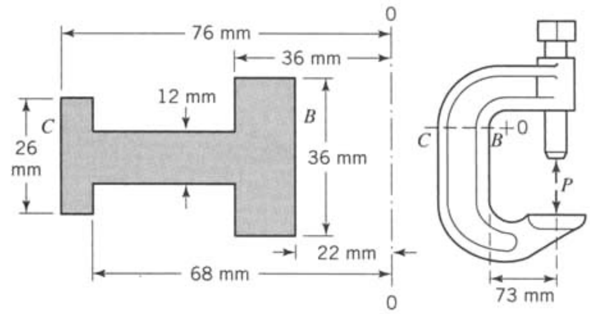

FIGURE P9.20

9.21. Determine the radial stress at the junction of the web and inner flange of the curved beam portion of the clamp in Problem 9.20. Neglect stress concentrations.

Section 9.5

9.22. If moment M_x and axial force N are applied simultaneously, the strain-energy density resulting from these two actions is

$$dU = \frac{1}{2}M_x \omega \, d\theta + \frac{1}{2}N \bar{\epsilon}_{\theta\theta} R \, d\theta$$

where ω is given by Eq. 9.10 and $\bar{\epsilon}_{\theta\theta}$ is found from Eq. 9.3 with $r = R$. Using this expression for strain-energy density, derive Eq. 9.31.

9.23. The curved beam in Figure P9.23 is made of a steel (E = 200 GPa) that has a yield stress Y = 420 MPa. Determine the magnitude of the bending moment M_Y required to initiate yielding in the curved beam, the angle change of the free end, and the horizontal and vertical components of the deflection of the free end.

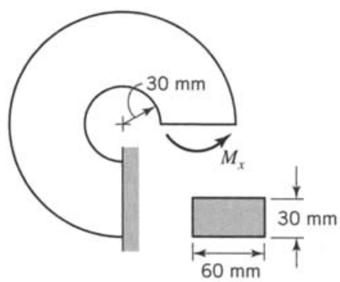

FIGURE P9.23

9.24. Determine the deflection of the curved beam in Problem 9.7 at the point of load application. The curved beam is made of an aluminum alloy for which E = 72.0 GPa and G = 27.1 GPa. Let k = 1.3.

9.25. The triangular cross section curved beam in Problem 9.12 is made of steel (E = 200 GPa and G = 77.5 GPa). Determine the separation of the points of application of the load. Let k = 1.5.

9.26. Determine the deflection across the center of curvature of the cast iron curved beam in Problem 9.17 for P = 126 kN. E = 102.0 GPa and G = 42.5 GPa. Let k = 1.0 with the area in shear equal to the product of the web thickness and the depth.

Section 9.6

9.27. The ring in Figure P9.27 has an inside diameter of 100 mm, an outside diameter of 180 mm, and a circular cross section. The ring is made of steel having a yield stress of Y = 520 MPa. Determine the maximum allowable magnitude of P if the ring has been designed with a factor of safety SF = 1.75 against initiation of yielding.

9.28. If E = 200 GPa and G = 77.5 GPa for the steel in Problem 9.27, determine the deflection of the ring for a load P = 60 kN. Let k = 1.3.

9.29. An aluminum alloy ring has a mean diameter of 600 mm and a rectangular cross section with 200 mm thickness and a depth of 300 mm (radial direction). The ring is loaded by

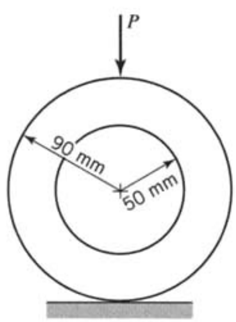

FIGURE P9.27

diametrically opposed radial loads $P = 4.00$ MN. Determine the maximum tensile and compressive circumferential stresses in the ring.

9.30. If $E = 72.0$ GPa and $G = 27.1$ GPa for the aluminum alloy ring in Problem 9.29, determine the separation of the points of application of the loads. Let $k = 1.5$.

9.31. The link in Figure P9.31 has a circular cross section and is made of a steel having a yield stress of $Y = 250$ MPa. Determine the magnitude of P that will initiate yield in the link.

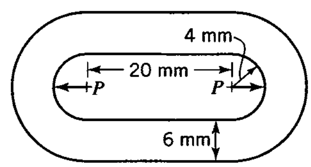

FIGURE P9.31

Section 9.7

9.32. Let the curved beam in Figure 9.10 have a rectangular cross section with depth h and width b. Show that the ratio of the bending moment M for fully plastic load P_P to the fully plastic moment for pure bending $M_P = Ybh^2/4$ is given by the relation

$$\frac{M}{M_P} = \frac{4D}{h}\sqrt{1 + \frac{4D^2}{h^2} - \frac{8D^2}{h^2}}$$

9.33. Let the curved beam in Problem 9.5 be made of a steel that has a flat-top stress–strain diagram at the yield stress $Y = 430$ MPa. From the answer to Problem 9.5, the load that initiates yielding is equal to $P_Y = SF(P) = 6.05$ kN. Since $D = 3h$, assume $M = M_P$ and calculate P_P. Determine the ratio P_P/P_Y.

9.34. Let the steel in the curved beam in Example 9.8 be elastic–perfectly plastic with yield stress $Y = 280$ MPa. Determine the fully plastic moment for the curved beam. Note that the original cross section must be used. The distortion of the cross section increases the fully plastic moment for a positive moment.

REFERENCES

AMERICAN INSTITUTE OF TIMBER CONSTRUCTION (AITC) (1994). *Timber Construction Manual*, 4th ed. New York: Wiley.

ANDERSON, C. G. (1950). Flexural Stresses in Curved Beams of I- and Box Sections. Presented to Inst. of Mech. Engineers, London, Nov. 3.

BLEICH, H. (1933). Die Spannungsverteilung in den Gurtungen gekrümmter Stabe mit T- und I-formigem Querschnitt. *Der Stahlblau, Beilage zur Zeitschrift, Die Bautechnik*, **6**(1): 3–6.

BROUGHTON, D. C., CLARK, M. E., and CORTEN, H. T. (1950). Tests and Theory of Elastic Stresses in Curved Beams Having I- and T-Sections. *Exper. Mech.*, **8**(1): 143–155.

MCWHORTER, J. C., WETENKAMP, H. R., and SIDEBOTTOM, O. M. (1971). Finite Deflections of Curved Beams. *J. Eng. Mech. Div., Proc. ASCE*, **97**: 345–358.

TIMOSHENKO, S. (1923). Bending Stresses in Curved Tubes of Rectangular Cross-Section. *Trans. ASME*, **45**: 135–140.

TIMOSHENKO, S., and GOODIER, J. (1970). *Theory of Elasticity*, 3rd ed. New York: McGraw-Hill.

WANG, C. C. (1985). A Unified Algorithm for Accurately Sizing Straight and Curved Beam Sections to Allowable Stress Limits. Presented at ASME Des. Eng. Div. Conf. and Exhibit on Mech. Vibration and Noise, Cincinnati, OH, Sept. 10–13, Paper 85-DET-102.